Genome-wide DNA methylation profiling identifies a folate-sensitive region of differential methylation upstream of *ZFP57*-imprinting regulator in humans

Manori Amarasekera,* David Martino,[†,‡,§] Sarah Ashley,[†,‖] Hani Harb,[¶] Dörthe Kesper,[¶] Deborah Strickland,[#] Richard Saffery,[†,‡] and Susan L. Prescott*,[1]

*School of Paediatrics and Child Health, University of Western Australia, Perth, Western Australia, Australia; [†]Cancer and Disease Epigenetics Group, Murdoch Children's Research Institute, Melbourne, Victoria, Australia; [‡]Department of Paediatrics, University of Melbourne, Melbourne, Victoria, Australia; [§]Centre for Food and Allergy Research, Melbourne, Victoria, Australia; [‖]Institute for Medical Research, Monash University, Melbourne, Victoria, Australia; [¶]Institute of Laboratory Medicine, Pathobiochemistry, and Molecular Diagnostics, Philipps University, Marburg, Germany; and [#]Telethon Institute for Child Health Research, Perth, Western Australia, Australia

ABSTRACT **Folate intake during pregnancy may affect the regulation of DNA methylation during fetal development. The genomic regions in the offspring that may be sensitive to folate exposure during *in utero* development have not been characterized. Using genome-scale profiling, we investigated DNA methylation in 2 immune cell types ($CD4^+$ and antigen-presenting cells) isolated from neonatal cord blood, selected on the basis of *in utero* folate exposure. High-folate (HF; $n=11$) and low-folate (LF; $n=12$) groups were selected from opposite extremes of maternal serum folate levels measured in the last trimester of pregnancy. A comparison of these groups revealed differential methylation at 7 regions across the genome. By far, the biggest effect observed was hypomethylation of a 923 bp region 3 kb upstream of the *ZFP57* transcript, a regulator of DNA methylation during development, observed in both cell types. Levels of H3/H4 acetylation at *ZFP57* promoter and *ZFP57* mRNA expression were higher in $CD4^+$ cells in the HF group relative to the LF group. Hypomethylation at this region was replicated in an independent sample set. These data suggest that exposure to folate has effects on the regulation of DNA methylation during fetal development, and this may be important for health and disease.—Amarasekera, M., Martino, D., Ashley, S., Harb, H., Kesper, D., Strickland, D., Saffery, R., Prescott, S. L. Genome-wide DNA methylation profiling identifies a folate-sensitive region of differential methylation upstream of *ZFP57*-imprinting regulator in humans. *FASEB J.* 28, 4068–4076 (2014). www.fasebj.org**

Key Words: epigenetics · developmental programming · neonate · antigen-presenting cells · T cells

DNA METHYLATION IS A KEY epigenetic mechanism controlling fetal growth and development (1). Animal studies suggest that dietary intake of nutrients involved in 1-carbon metabolism, such as folic acid, during pregnancy can influence DNA methylation in the developing offspring, which may lead to an altered phenotype (2–4).

In humans, periconceptional supplementation with folic acid is routinely recommended to prevent the occurrence of neural tube defects (5). However, emerging data have linked folic acid intake during pregnancy with disease outcomes in the offspring, including atopic dermatitis (6, 7) childhood wheeze (8), and asthma (9). Parallel investigations into potential underlying epigenetic mechanisms have mostly focused on genomic regions surrounding imprinted genes that regulate growth and development. Several studies have now reported variations in DNA methylation at these regions in offspring exposed to periconceptional folic acid. Steegers-Theunissen *et al.* (10) reported the average methylation of the imprinted insulin-like growth factor 2 (*IGF2*) differentially methylated region (DMR) was 4.5% higher in infants whose mothers reported periconceptional intake of folic acid at a dose of 400 μg/d compared with infants whose mothers did not take folic acid. Another study reported that average methylation at the imprinted *H19* DMR in cord blood leukocytes was significantly lower in neonates of mothers who took

Abbreviations: APC, antigen-presenting cell; ChIP, chromatin immunoprecipitation; CMBC, cord blood mononuclear cell; DMP, differentially methylated position; DMR, differentially methylated region; fDMR, folate-sensitive differentially methylated region; H3, histone H4, histone 4; HF, high folate; IGF2, insulin-like growth factor 2; LF, low folate

[1] Correspondence: School of Paediatrics and Child Health, University of Western Australia, P.O. Box D184, Princess Margaret Hospital, Perth, WA 6001, Australia. E-mail: susan.prescott@uwa.edu.au

doi: 10.1096/fj.13-249029

This article includes supplemental data. Please visit *http://www.fasebj.org* to obtain this information.

0892-6638/14/0028-4068 © FASEB

folic acid either before or during pregnancy compared to neonates of mothers who reported no folic acid intake as ascertained from self-administered questionnaires (11). Together, these findings suggest a complex relationship between maternal folic acid intake and DNA methylation levels at imprinted genes and variation in folate exposure during development may have effects on neonatal growth and susceptibility to diseases in later life (12). Adding another layer of complexity to the association between folate and methylation profile is that the effects of folate exposure appear to be tissue specific. Chang *et al.* (13) investigated the influence of maternal serum folate on DNA methylation in 18- to 28-wk-old fetuses following termination of pregnancy for fetal anomalies. They found a positive correlation between the levels of DNA methylation and maternal serum folate levels in brain tissue but not in other tissues, indicating that exposure to folic acid during pregnancy may have tissue-specific effects in the developing offspring.

Very few human studies have used a genome-wide approach in mapping the DNA methylation changes at birth that are associated with variation in folate exposure during pregnancy (14, 15). The concern has therefore been such that changes in epigenetic marks in fetal epigenome induced by variations in maternal folic acid intake may have long-term health consequences in accordance with the developmental origin of health and disease hypothesis (16). To advance this area, we conducted a genome-scale profiling of 450,000 CpG sites in 2 key neonatal immune cell types [$CD4^+$ T cells and antigen-presenting cells (APCs)] purified from cord blood. We chose to study 2 cell types representing distinct hematopoietic lineages with well-defined roles in regulating the host immune response to the environment (17).Notably, by using purified cell populations in this study, we were able to avoid potential confounding effects of cell heterogeneity that may affect the measured epigenetic changes (18). Neonates for this study were selected from the extremes of the maternal serum folate distribution curve from a Western Australian birth cohort. Using an explorative hypothesis-free approach coupled with an extreme of exposure design we have identified several folate-sensitive DMRs (fDMRs) in the genome.

MATERIALS AND METHODS

Selection of the study population

The study population included 23 neonates selected from a larger prospective birth cohort of mother-infant pairs recruited through the allergy research clinic in the Princess Margaret Hospital for Children (Perth, WA, Australia; ref. 7). Mothers were recruited during the last trimester (≥28 wk) of pregnancy, at which time maternal blood samples were collected; cord blood samples were subsequently collected at the time of birth. Peripheral blood mononuclear cells were harvested from blood samples within 12 h of collection according to standard protocols (19). Matched serum folate measurements were available for both maternal and cord blood for $n = 222$ mother-infant pairs. Extensive clinical and dietary data collected at recruitment through semiquantitative food frequency questionnaires and maternal antenatal and sociodemographic factors were also available.

The sample population was selected based on the following criteria: infants were "nonatopic" and otherwise healthy based on clinical assessments and skin-prick test to a range of inhalant and dietary allergens conducted at 12 mo. The high-folate (HF) and low-folate (LF) groups were defined according to the first and third quartiles from the distribution of maternal serum folate levels in conventional extremes of exposure design. Infants were excluded from the study if exposed to maternal smoking in pregnancy or if they had evidence of congenital birth defects. All study procedures were carried out in accordance with full institutional ethics.

Serum folate measurement

Folate levels were measured in maternal serum from blood samples collected during the last trimester of pregnancy, and neonatal serum folate was measured from cord blood samples using the Immulite 2000 competitive immunoassay platform (Siemans Medical Solutions Diagnostics, Flanders, NJ, USA).

Isolation of $CD4^+$ T cells

$CD4^+$ T cells were isolated from cord blood mononuclear cells (CBMCs) using a 2-stage positive isolation strategy with magnetic Dynal beads (Invitrogen, Mount Waverley, VIC, Australia). CBMCs were incubated with $CD8^+$ magnetic beads (Invitrogen) as per the recommended protocol, and the $CD8^-$ fraction was then incubated with $CD4^+$ magnetic beads as per the recommended protocol. Routine purity tests were conducted by flow cytometry using antibodies CD19-FITC, CD3-PE, CD8-PerCP, CD11c-PE Cy7, CD4-APC, and CD14-APC Cy7 (BD Biosciences, San Jose, CA, USA) and appropriate concentration matched istoype controls. $CD4^+$ cell purities ranged from 89 to 96% pure. A fraction of isolated $CD4^+$ cells were frozen with 15% dimethyl sulfoxide in heat-inactivated fetal calf serum and stored in liquid nitrogen until transported to Marburg, Germany, for chromatin immunoprecipitation (ChIP) analysis. The rest of the $CD4^+$ T cells were lysed with RLT buffer containing 2-mercaptoethanol (Qiagen Allprep kit; Qiagen, Chadstone, VIC, Australia)) and stored at −80°C until genomic DNA was extracted for methylation analysis.

Isolation of APCs

$CD3^-CD19^-CD14^{+/-}$ $CD11c^+$ $HLADR^+$ myeloid APCs were sorted from $CD4^+$- and $CD8^+$-depleted cell fractions using an FACSAria instrument and FACSDiva software (BD Biosciences, San Jose, CA, USA).

Nucleic acid extraction

Genomic DNA and mRNA were copurified from $CD4^+$ T cells and APCs using Qiagen Allprep kits according to manufacturer's instructions.

DNA methylation analysis

A total of 500 ng of purified genomic DNA from each cell type was bisulfite converted using the MethylEasy Xceed kit from Human Genetic Signatures (North Ryde, NSW, Australia). Successful bisulfite conversion was evaluated for all samples using an in-house bisulfite-specific PCR. Bisulfite DNA was sent to the Australian Genome Research Facility (Parkville, VIC, Australia) for labeling, staining, and hybridization to Illumina Human Methylation 450 arrays (Illumina,

San Diego, CA, USA). Raw iDAT files were processed using the Minfi package from the Bioconductor Project (Fred Hutchinson Cancer Research Center, Seattle, WA, USA; http://www.bioconductor.org) in the R statistical environment (http://cran.r-project.org/). The Minfi package was used for array preprocessing using the stratified quantile normalization method. Technical bias attributable to different probe chemistries between type 1 and type II probes were adjusted in this procedure. Probes with a detection value of $P > 0.01$ in ≥1 sample were removed. Probes on the X and Y chromosomes were removed to eliminate gender bias. Probes previously demonstrated to potentially cross-hybridize nonspecifically in the genome were removed (20). Probes containing a polymorphic single-nucleotide polymorphism at the single-base extension site with a minor allele frequency of <0.05 were removed. The $\log_2$ ratio for methylated probe intensity to unmethylated probe intensity, the *M* value, was subsequently derived and used for statistical inference. Values of β were derived from intensities as defined by the ratio of methylated to unmethylated probes given by $\beta = M/(U/M \times 100)$ and were used to complement the *M* value as a measure of effect size. Cluster analysis was used in conjunction with the chipwide medians of the methylated and unmethylated channels to identify any outlying samples, and 1 sample was removed from the data set.

Quantitative PCR

First-strand cDNA was generated by reverse transcription of 500 ng total RNA/sample with random hexamers using SuperScript VILO (Invitrogen) according to the manufacturer's instructions. cDNA was diluted 1:5 in RNase-free water for gene expression analysis. Relative quantitation of gene expression was performed using predesigned TaqMan assays (Applied Biosystems, Foster City, CA, USA) for *ZFP57* on the ABI 7300 real-time PCR system (Applied Biosystems) in triplicate. All samples were normalized to the housekeeping gene PPIA. Absolute levels of *ZFP57* mRNA expression were low and not measurable for 8/21

TABLE 1. *Population characteristics of the mothers and infants in the discovery cohort*

Characteristic	High-folate group	Low-folate group	*P*
n	11	12	
Mothers at recruitment			
Age (yr)	31.9 ± 1.25	32.1 ± 0.82	0.95
History of allergic disease [*n* (%)]	8 (73)	8 (67)	0.75
Asthma [*n* (%)]	4 (36)	3 (25)	0.55
Hay fever [*n* (%)]	5 (45)	7 (58)	0.54
Eczema [*n* (%)]	5 (45)	4 (33)	0.55
IgE-mediated food allergy [*n* (%)]	1 (9)	1 (8)	0.95
Sensitization [*n* (%)]	9 (82)	10 (83)	0.92
Had tertiary education [*n* (%)]	8 (73)	11 (92)	0.23
Not exposed to passive smoke (%)	36	33	0.44
Infants			
Male [*n* (%)]	4 (36)	5 (42)	0.80
Gestation (wk)	39.7 (0.3)	39.2 (0.3)	0.28
Delivery method			
Vaginal [*n* (%)]	6 (54)	4 (40)	
Caesarean section [*n* (%)]	5 (45)	6 (60)	0.51
Neonatal growth parameters			
Birth weight (g)	3420.3 ± 79	3570.9 ± 128	0.43
Length (cm)	50.2 ± 0.5	49.9 ± 0.9	0.79
Head circumference (cm)	35.0 ± 0.3	35.6 ± 0.5	0.34
Serum folate			
Maternal serum folate level at recruitment (nM)	74.59 ± 6.1	16.8 ± 1.6	<0.001*
Cord serum folate (nM)	78.15 ± 5.1	36.4 ± 2.3	<0.001*
Cord serum vitamin D (nM)	59.9 ± 7.8	39.0 ± 5.7	0.04*
Maternal daily folic acid intake from supplements (from questionnaire data;μg DFE/d)	730.9 ± 127	236.6 ± 120.7	0.006*
Maternal daily intake from diet (from semiquantitative food frequency questionnaire)			
Folate (μg DFE/d)	310.7 ± 36.4	199.2 ± 33.7	0.02*
Vitamin D (μg)	3.8 ± 0.8	4.4 ± 1.7	0.56
Total energy (kcal)	2271.9 ± 126	2019.2 ± 294	0.71
Protein (g)	88.9 ± 5.2	83.7 ± 12.8	0.71
Total fat (g)	88.8 ± 8.4	79.4 ± 12.9	0.37
Copper (mg)	2.2 ± 0.1	1.8 ± 0.3	0.22
Zinc (mg)	12.0 ± 0.8	10.5 ± 1.3	0.22
Retinol (μg)	512.3 ± 84	538.4 ± 157	0.56
Vitamin B6 (mg)	2.0 ± 0.2	1.5 ± 0.3	0.22
Vitamin B12 (mg)	3.4 ± 0.4	3.7 ± 1.0	0.96
Alcohol (g)	1.8 ± 0.8	1.8 ± 1.1	0.78
Coffee (g)	84.2 ± 58.8	144.9 ± 69.2	0.25
Vitamin A (μg)	1390.2 ± 106	1215.4 ± 268	0.5

Values are means ± SE or as indicated. DFE, dietary folate equivalent. Statistical comparisons by χ^2 and Mann-Whitney *U* tests. *$P < 0.05$.

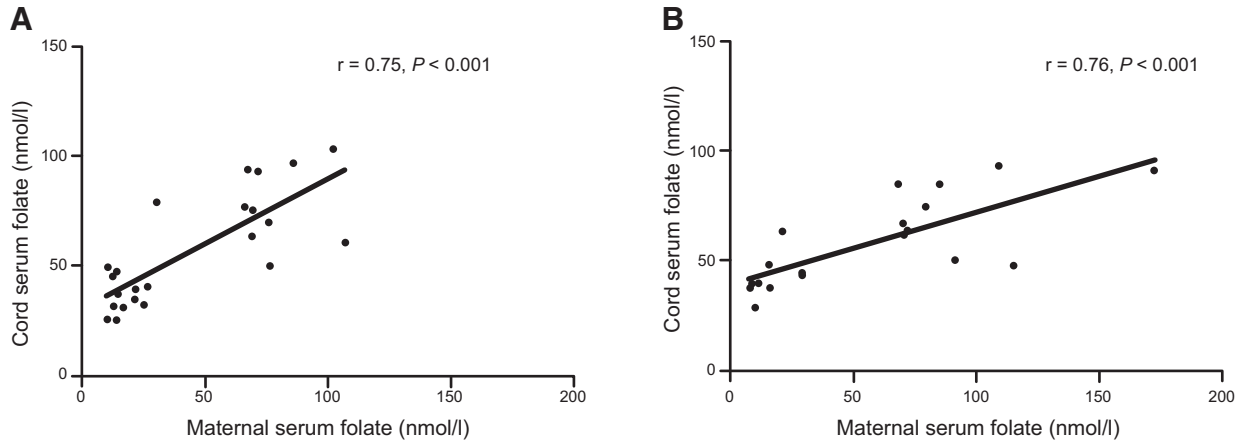

Figure 1. Relationship between maternal serum folate levels and cord serum folate levels. *A*) Samples in the discovery cohort. *B*) Samples in the replication cohort. Graphs show correlation plots between maternal serum folate levels measured at the recruitment visit during the third trimester and cord serum folate levels collected at birth.

individuals, and these were assigned a maximum C_T value of 45 for statistical analysis and interpretation at the group level.

Data analysis

Characteristics of genome-wide DNA methylation were assessed by principal components analysis in the presence of potential confounding factors. The first 15 principal components capturing >65% of the total variance were derived and tested for associations with clinical variables. Clinical variables associated with variation in DNA methylation are provided in Supplemental Data and were included as covariates in regression modeling. To identify DMRs, we used the dmrFind algorithm in the Charm package (Bioconductor Project) under the default settings with the cluster marker function. This algorithm combines surrogate variable analysis (21) for modeling unexplained variability due to batch effects or covariates, with regression modeling fitted to the entire dataset in the presence of covariates and surrogate variables (22). Comparisons are made at the regional level as opposed to single-CpG analysis, whereby methylation estimates are smoothed over spatial blocks accounting for correlation between nearby CpGs. Ontology enrichment analysis was performed using the Genomic Regions Enrichment of Annotations Tool (GREAT) ontology tool (Stanford University, Stanford, CA, USA; http://bejerano.stanford.edu/great/public/html/) under the default basal plus extension settings. Significant ontologies are reported as raw $-\log_{10}$ binomial $P < 0.05$.

Validation of array targets

Target validation was performed using the Sequenom EpiTyper platform (Sequenom, San Diego, CA, USA) in triplicate. Amplicons were designed using the Sequenom EpiDesigner software (http://www.epidesigner.com/). Amplification conditions were as follows: 95°C for 10 min, 95°C for 15 s, 56°C for 30 s, 72°C for 2 min for 5 cycles, 95°C for 10 s, 60°C for 30 s, 72°C for 1 min 30 s for 30 cycles, 72°C for 7 min. The target sequences of the chromosome 6 fDMR were aggaagagagGAGGATTTTAGAGGTTGGAAGTTTT (left) and cagtaatacgactcactatagggagaaggctCCCTCTCATCTAAATCAAAAAACAC (right).

Histone 3 (H3) and histone 4 (H4) acetylation analysis

Using a validated ChIP analysis for H3/H4 acetylation in human immune cells, we analyzed the levels of H3/H4

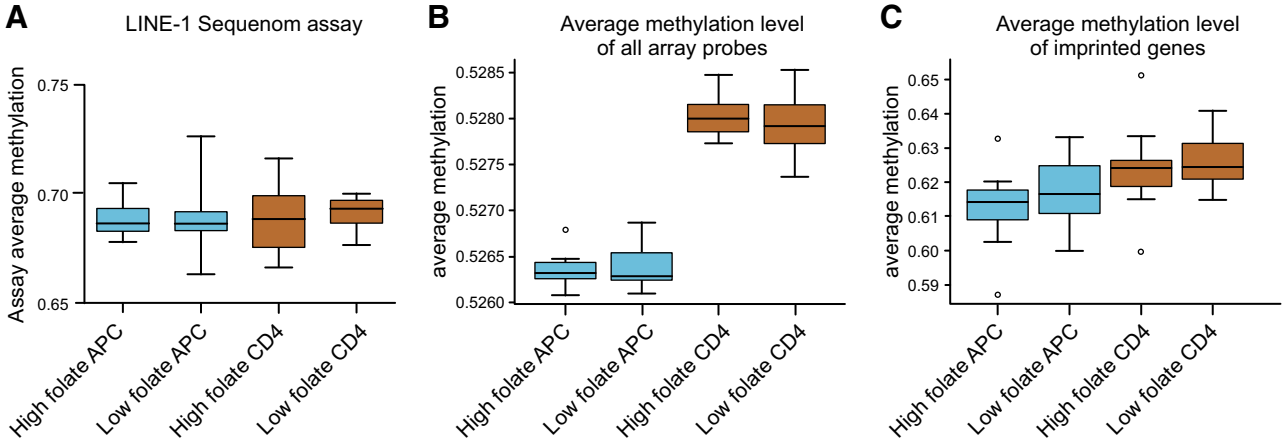

Figure 2. Analysis of global patterns of DNA methylation between folate groups. *A*) Sequenom EpiTyper analysis of LINE-1 DNA methylation levels. *B*) Mean methylation level for all somatic probes on the Illumina methylation 450k array. *C*) Mean methylation levels specifically for probes targeting imprinted genes on the Illumina methylation array. All box plots show means with range.

acetylation at selected loci. In brief, DNA-histone interactions in isolated $CD4^+$ T cells were first cross-linked with 1% formaldehyde. Subsequently, chromatin was sonicated to achieve the optimal DNA length for the immunoprecipitation, which was done using antibodies against acetylated H3 and H4 (Millipore, Darmstadt, Germany). IgG mock control was bought from Abcam (San Francisco, CA, USA). Quantitative PCR was performed to measure the precipitated DNA of investigated loci. Primers were designed for known transcripts of *ZFP57* and are as follows: ZFP57-001 distal (ZFP57_1D) caccaccggctaacttttgt (forward) and cctgggcaaaaagagtgaaa (reverse), ZFP57-002 proximal (ZFP57_2P) cccaggctggtgttgttact (forward) and ggtttgatgtggcttcctgt (reverse), ZFP57-002 distal (ZFP57_2D) catggaagagatcttagagagtg (forward) and acctaatgcagagatgctaaataa (reverse).

RESULTS

Clinical characteristics of the cohort

Maternal serum folate levels ranged from 4.1 to 172.0 nM in the cohort from which the study samples were derived, with first and third quartiles 25.6 and 50.5 nM, respectively. The HF and LF groups were identified from this cohort and defined according to the first and third quartiles from the distribution of maternal serum folate levels in conventional extremes of exposure design. The mean maternal serum folate measurement at recruitment was 74.6 and 16.8 nM in the HF and LF group ($P<0.001$), with corresponding cord blood serum levels of 78.2 and 36.4 nM ($P<0.001$), respectively (**Table 1**). There were no significant differences in the key neonatal parameters between HF and LF groups, with the exception of folate intake during pregnancy (either as food, $P=0.02$, or as supplement, $P=0.006$), and cord blood serum vitamin D levels ($P=0.04$), which were found to be significantly higher in the HF group (Table 1). Based on this, all subsequent analysis was adjusted for any potential effects of vitamin D. There was a significant linear relationship between maternal serum folate and cord blood folate levels in the sample population ($r=0.75$, $P<0.001$; **Fig. 1*A***).

Characteristics of genome-scale DNA methylation profiles

Genome-scale DNA methylation data were generated from 2 blood cell types representing both the innate (APC) and the adaptive ($CD4^+$) immune cell compartments. These cell types play a well-defined role in antigen presentation and processing and mediation of effector immune cell responses. Principal components analysis on β-methylation values was used to explore variation in neonatal epigenetic profiles. The most substantial source of variation in the data set was attributable to cell type (APC or $CD4^+$). Multidimensional scaling and hierarchical clustering of samples showed widespread differences between cell types reflecting the alternative lineages of APC (myeloid origin) and $CD4^+$ cells (lymphoid origin) (Supplemental Fig. S1*A*). Differential analysis of $CD4^+$ and APC cells revealed a signature of 13,424 CpG sites (~3.5% of the

TABLE 2. *DMRs according to folate status, irrespective of cell type*

DMR	Chromosome	Start	End	Size (bp)	Probes	DM		HF *vs.* LF	Gene association	Function
						Average	Maximum			
1	6	29,648,161	29,649,084	923	19	0.19	0.28	Hypomethylated	ZFP57 (−3692)	Maintenance of DNA methylation and genomic imprinting
2	17	37,123,638	37,123,949	311	8	−0.08	−0.12	Hypermethylated	LASP1 (+97,682)	Regulation of dynamic actin-based, cytoskeletal activities
3	1	76,189,707	76,190,008	301	5	−0.13	−0.23	Hypermethylated	ACADM (−185)	Mitochondrial fatty acid β-oxidation pathway
4	8	144,120,106	144,120,706	600	7	0.08	0.10	Hypomethylated	LY6E (+20,504)	Lymphocyte antigen complex
5	1	228,075,423	228,075,749	326	5	−0.10	−0.13	Hypermethylated	WNT9A (+60,090)	Development and cell fate
6	21	47,604,052	47,604,654	602	5	0.09	0.11	Hypomethylated	C21orf56 (+20)	Unknown
7	2	202,901,045	202,901,470	425	5	−0.08	−0.11	Hypermethylated	FZD7 (+1948)	Wnt protein binding

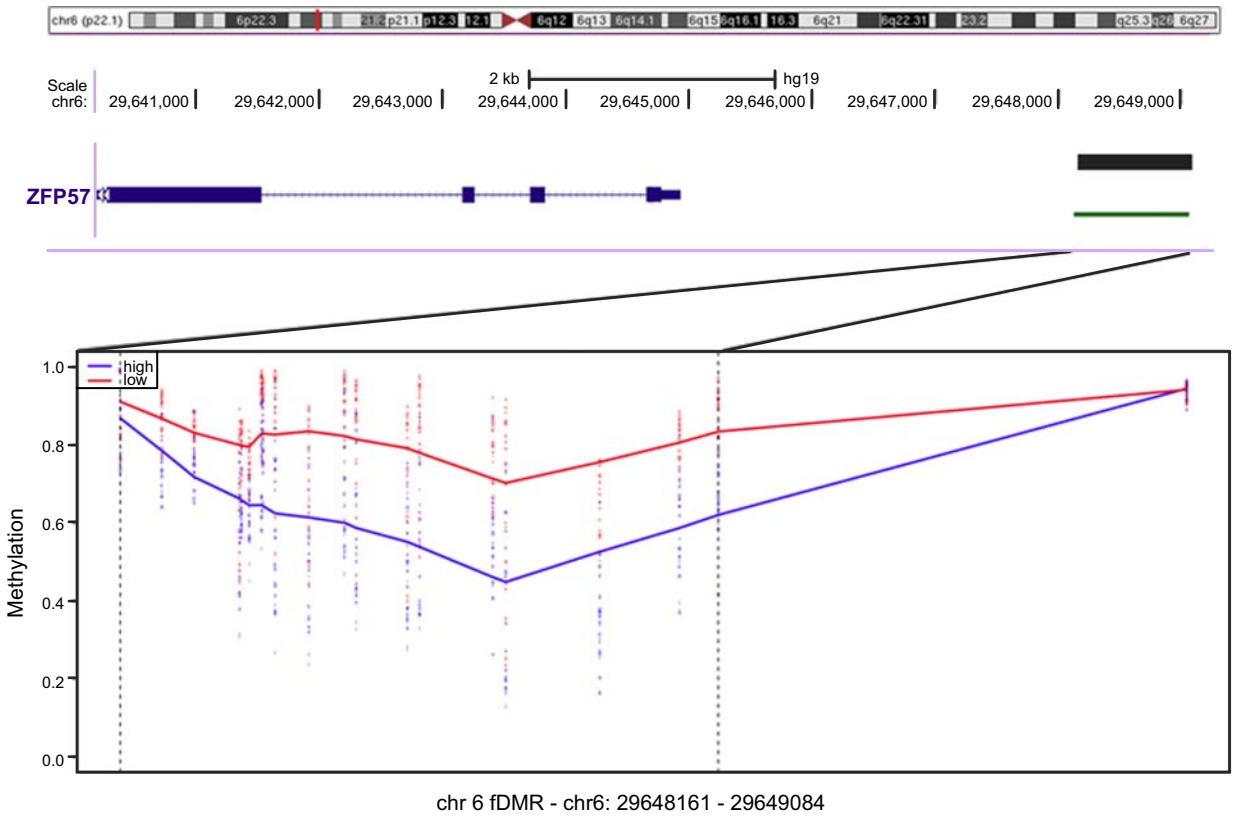

Figure 3. fDMR in chromosome 6 with the smoothed β methylation values for LF (red) and HF (blue) groups, averaged for both cell types. Location and size of this DMR are shown in the genome browser track above the sliding window. Ideogram track shows the location of this region on chromosome 6.

CpG sites measured) that differed by a minimum Δ_β value of ≥20% and reached genome-wide significance (5048 hypermethylated, 8376 hypomethylated sites). Localization of these sites to functional regions in the genome revealed the majority of these differentially methylated positions (DMPs) were localized to gene bodies as opposed to promoters, and overlapped with flanking regions of CpG islands (CpG island shore and shelves), or were found in open sea regions (not island associated) (Supplemental Fig. S1*B*). The DMPs were significantly enriched for genes involved in leukocyte function and antigen-mediated pathways (binomial $P<0.05$; data not shown). Birth mode, maternal serum folate levels, folate status (high or low), and serum vitamin D levels were included as covariates in data modeling.

Differential methylation according to folate status

We first examined general features of DNA methylation between folate groups at several regions in the genome, including repeat elements, nonrepeat CpGs, and imprinted genes. Folate status was not associated with changes in DNA methylation levels at long interspersed nucleotide element-1 repeat elements in the genome of either cell type (**Fig. 2*A***). The average level of DNA methylation in the genome as measured by the mean of all CpGs on the array did not differ according to serum folate status in either cell type (Fig. 2*B*). Similarly, average and total levels of DNA methylation levels across CpG sites targeting known imprinted genes did not vary according to folate status (Fig. 2*C*). Collectively these data suggest the general features of the DNA methylome in the offspring are similar regardless of folate exposure during pregnancy.

Next the methylation values for all probes were regressed on folate status (HF or LF), adjusting for known covariates including cell type, to identify fDMRs in the methylome. We adopted a sliding-windows approach that is more powerful than single-CpG analysis to identify broad DMRs consistent in both cell types by computing smoothed estimates of regionally associated probes (22). Seven candidate regions, defined as an average of ≥4 consecutively differentially methylated CpG sites, were identified in this analysis (**Table 2**) including a 923 bp region in chromosome 6 of substantial hypomethylation in the HF group 3 kb upstream of the *ZFP57* gene (**Fig. 3**).

Validation of candidate loci and functional assessment of *ZFP57*

We measured DNA methylation levels in $CD4^+$ from the initial discovery cohort of samples interrogated by the DNA microarray using the Sequenom EpiTyper platform as a gold-standard technology. We designed an amplicon spanning a 321 bp region capturing 8 CpG sites in the chromosome 6 DMR upstream of *ZFP57* identified by HM450 analysis as broadly hypomethylated in HF samples. Data from the EpiTyper were in

agreement with observations from the array with hypomethylation observed in HF relative to LF groups (**Fig. 4*A***). To determine whether hypomethylation at this fDMR was indeed associated with the functional activity of the distal *ZFP57* gene, we measured both mRNA gene expression and histone acetylation in the same $CD4^+$ samples that were analyzed by microarray. A TaqMan PCR amplicon and an in-house histone H3/H4 acetylation assay targeted to the transcriptional start site of *ZFP57* were designed. A comparison of HF and LF groups revealed increased levels of histone H3 and H4 acetylation at *ZFP57,* a marker of increased transcriptional activity (Fig. 4*B*). In general absolute mRNA expression levels were low but relative differences were in the order of 4-fold between groups which was statistically significant (Fig. 4*C*). Collectively, these lines of evidence suggest a functional role for observed differences in DNA methylation associated with *ZFP57*.

Assessment of reproducibility in an independent set of samples

An independent sample population was next drawn from the source cohort in order to determine the potential reproducibility of the findings from our initial discovery cohort. We sampled an additional set of 19 samples from the first and third quartiles of the maternal serum folate distribution curve from the source population. The characteristics of these additional samples were similar to the discovery cohort, including a linear relationship between maternal serum folate levels and cord serum folate levels (r=0.76, P<0.001; Fig. 1*B*), but with the notable exception that vitamin D levels were not different in this group (P=0.2). Both $CD4^+$ and APC populations were purified from cord blood as described previously. In agreement with data obtained from the discovery cohort, levels of DNA methylation were consistently lower at the *ZFP57* fDMR in samples from the HF group (**Fig. 5**).

DISCUSSION

The folic acid metabolic pathway plays a critical role in fetal development (23), yet its effects on regulation of fetal DNA methylation and gene expression are incompletely understood. In this study, we investigated the

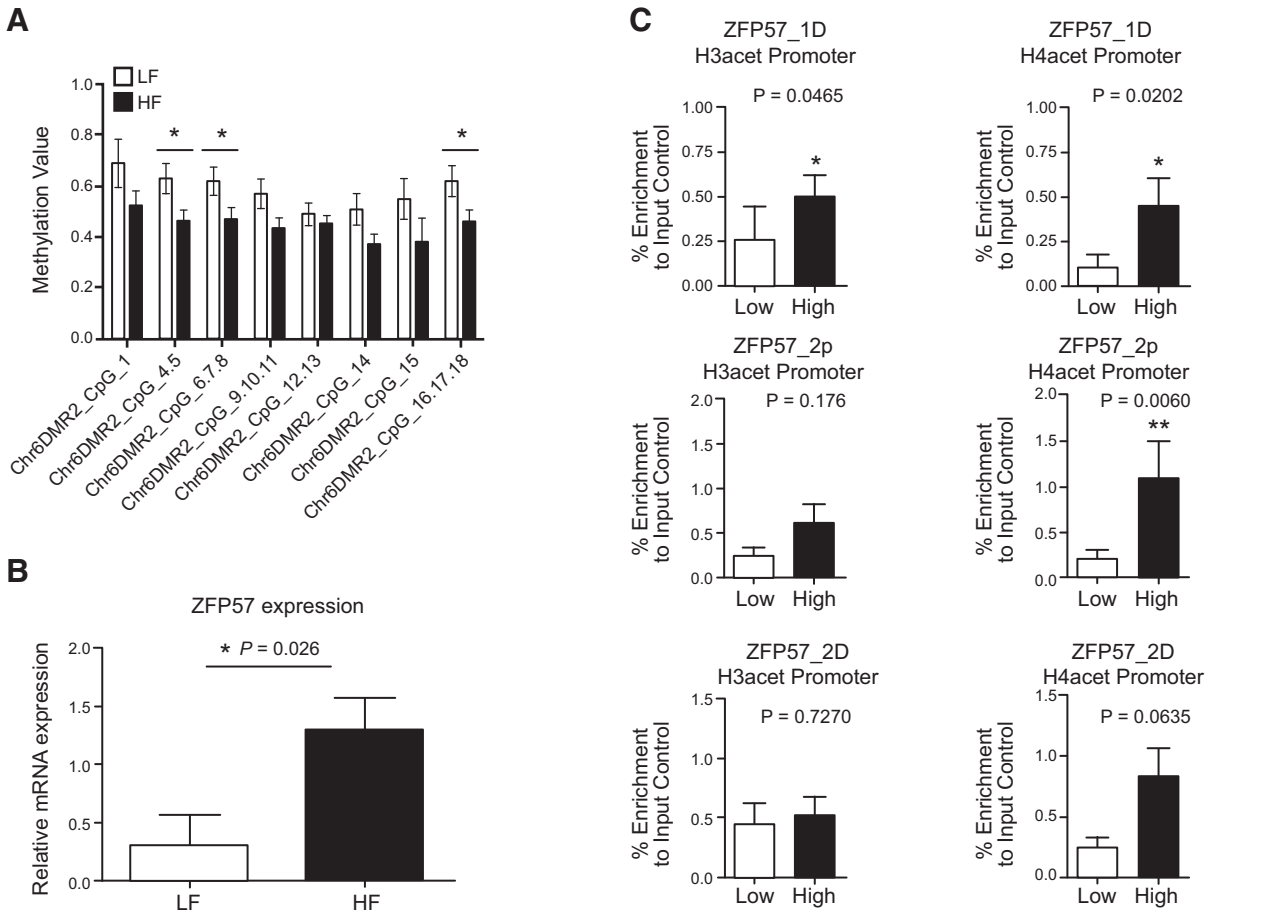

Figure 4. Validation data of chromosome 6 fDMR and functional assessment of *ZFP57* in $CD4^+$ cells. *A*) Consistent with findings from the Illumina array, data from Sequenom EpiTyper platform showing the trend of lower methylation in HF group and higher methylation in LF group. *B*) mRNA expression of *ZFP57* in $CD4^+$ cells shows an up-regulation of the gene in HF group. *C*) Levels of H3 and H4 acetylation at the *ZFP57* promoter region are higher in the HF group, indicating a more open chromatin state in this group. Details of the primer sequences are given in Supplemental Table S1.

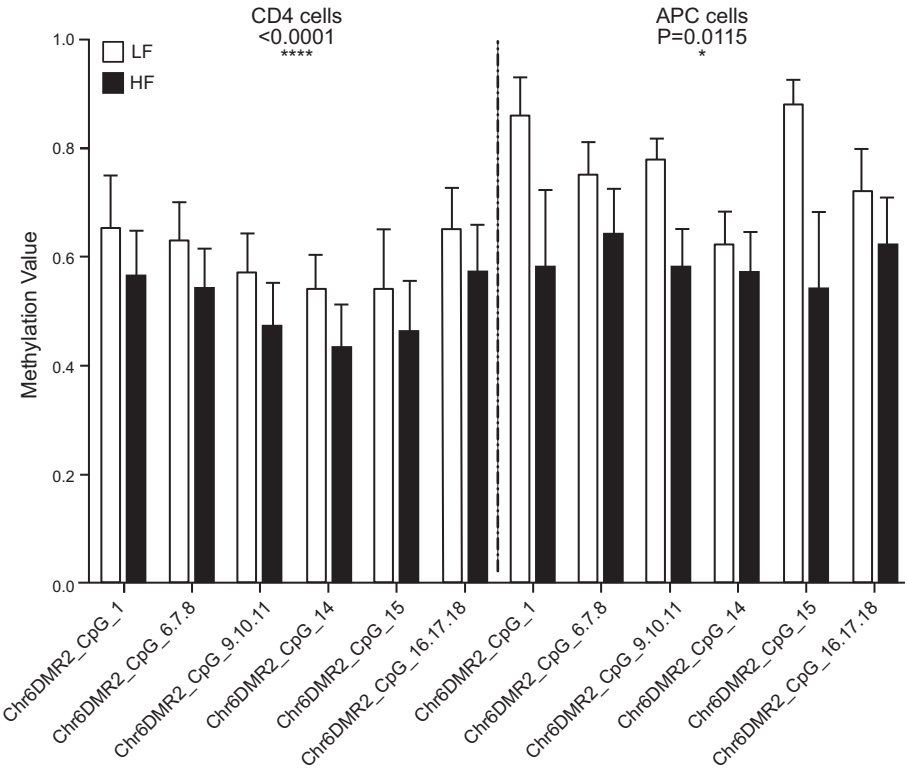

Figure 5. Sequenom Epityper analysis of DNA methylation at the chromosome 6 fDMR in an independent set of samples (n=19). Data show mean ± SE DNA methylation level at each CpG site. Statistics represent paired 2-tailed t test for average DNA methylation level across all 8 CpG sites (assay average).

effects of third-trimester maternal folate status on the DNA methylation profile of neonatal immune cells, with a view to identifying fDMRs in the genome. We began with a hypothesis-free discovery approach with subsequent replication of candidate loci in an independent set of samples. With this strategy, we have identified regions of the methylome that appear sensitive or responsive to folic acid status in pregnancy.

Using a genome-scale platform, we report several interesting features of the methylation landscape in neonates stratified by folate exposure in gestation. It is noteworthy that average DNA methylation levels, methylation levels at imprinted, and repeat elements of the genome appear unperturbed. Despite this, our analysis identified 7 folate-sensitive regions of methylation change in either direction. Folate plays a well-known role as a carrier of 1-carbon units that ultimately resulting in providing methyl groups to methylate DNA; hence, higher folate levels are expected to increase the levels of DNA methylation. However, many studies, both in humans and animals, have reported that high folate is associated with hypo- and hypermethylation, either globally or in a gene-specific manner (3, 11, 24). Ontology enrichment analysis of fDMRs suggests that these differences affect important genes involved in the regulation of DNA methylation during fetal development. Principal among these is *ZFP57*, a gene that plays a central role in regulation and maintenance of imprinting-associated DNA methylation (25, 26). Both data from the microarray and the EpiTyper platform suggest that HF exposure was associated with hypomethylation of a 923 bp region localized within a CpG dense cluster 3 kb upstream of the currently annotated *ZFP57* transcription start site. Analysis of histone acetylation profiles in the promoter of *ZFP57* and gene expression levels suggest hypomethylation at this fDMR is associated with markers of increased transcriptional activity. It is therefore tempting to speculate that a compensatory mechanism or a negative feedback loop may exist to regulate the activity of the *ZFP57* gene in response to folate exposure to stabilize DNA methylation levels at imprinting control regions. This assertion is based on the observation that imprinted regions targeted by the Illumina array did not differ according to folate status. However, within what range of folate exposure that this mechanism is biologically plausible and what other factors that may interfere with this compensatory mechanism is yet to be explored.

Accordingly, a recent study revealed that *ZFP57* is expressed in low but detectable levels in adult tissues, including peripheral blood mononuclear cells, and suggests that *ZFP57* may have other functions beyond imprinting establishment and maintenance (27). More recently, a study focusing on genes down-regulated in association with embryonic stem cell differentiation in mice identified *ZFP57*-mediated *IGF2* up-regulation in anchorage-independent growth of cancer cells (28). The researchers conclude that *ZFP57* acts as an oncogene in many cancer types. Further studies are needed to reconcile these findings.

Our 2-cell type screen suggests many of the fDMRs identified in this study are present more broadly throughout the hematopoietic compartment and, given that APCs and $CD4^+$ represent distinct lineages, suggest that folate driven effects on the epigenome have originated at the common hematopoietic progenitor stage. In addition, we identified a small number of cell-specific CpG sites associated with folic acid exposure; however, it is likely we are underpowered to characterize these smaller effects in sufficient detail.

Analysis of a second sample set drawn from the source population suggests that the findings reported here are likely to be reproducible to future investigators. Despite this, we have used an extremes of exposure design in which candidates were selected on the basis of serum folate levels, and therefore we cannot extend the effect sizes reported here to the general population. Nevertheless this study reports novel targets that represent viable research avenues for more large-scale population based studies in the future. These will be important to determine the extent to which periconceptional folate exposure modify the disease risk in offspring. FJ

R.S. is funded by an Australia National Health and Medical Research Council (NHMRC) Senior Research Fellowship and D.M. by an NHMRC Early Career Fellowship. Murdoch Children's Research Institute is supported by the Victorian government's Operational Infrastructure Scheme. All authors are members of the International Inflammation Network (inFLAME).

REFERENCES

1. Foley, D. L., Craig, J. M., Morley, R., Olsson, C. A., Dwyer, T., Smith, K., and Saffery, R. (2009) Prospects for epigenetic epidemiology. *Am. J. Epidemiol.* **169,** 389–400
2. Hollingsworth, J. W., Maruoka, S., Boon, K., Garantziotis, S., Li, Z., Tomfohr, J., Bailey, N., Potts, E. N., Whitehead, G., Brass, D. M., and Schwartz, D. A. (2008) In utero supplementation with methyl donors enhances allergic airway disease in mice. *J. Clin. Invest.* **118,** 3462–3469
3. Cho, C. E., Sanchez-Hernandez, D., Reza-Lopez, S. A., Huot, P. S., Kim, Y. I., and Anderson, G. H. (2013) High folate gestational and post-weaning diets alter hypothalamic feeding pathways by DNA methylation in Wistar rat offspring. *Epigenetics* **8,** 710–719
4. Waterland, R. A., and Jirtle, R. L. (2004) Early nutrition, epigenetic changes at transposons and imprinted genes, and enhanced susceptibility to adult chronic diseases. *Nutrition* **20,** 63–68
5. Lumley, J., Watson, L., Watson, M., and Bower, C. (2001) Periconceptional supplementation with folate and/or multivitamins for preventing neural tube defects. *Cochrane Database Syst. Rev.* **3,** CD001056
6. Kiefte-de Jong, J. C., Timmermans, S., Jaddoe, V. W., Hofman, A., Tiemeier, H., Steegers, E. A., de Jongste, J. C., and Moll, H. A. (2012) High circulating folate and vitamin B-12 concentrations in women during pregnancy are associated with increased prevalence of atopic dermatitis in their offspring. *J. Nutr.* **142,** 731–738
7. Dunstan, J. A., West, C., McCarthy, S., Metcalfe, J., Meldrum, S., Oddy, W. H., Tulic, M. K., D'Vaz, N., and Prescott, S. L. (2012) The relationship between maternal folate status in pregnancy, cord blood folate levels, and allergic outcomes in early childhood. *Allergy* **67,** 50–57
8. Haberg, S. E., London, S. J., Stigum, H., Nafstad, P., and Nystad, W. (2009) Folic acid supplements in pregnancy and early childhood respiratory health. *Arch. Dis. Child.* **94,** 180–184
9. Whitrow, M. J., Moore, V. M., Rumbold, A. R., and Davies, M. J. (2009) Effect of supplemental folic acid in pregnancy on childhood asthma: a prospective birth cohort study. *Am. J. Epidemiol.* **170,** 1486–1493
10. Steegers-Theunissen, R. P., Obermann-Borst, S. A., Kremer, D., Lindemans, J., Siebel, C., Steegers, E. A., Slagboom, P. E., and Heijmans, B. T. (2009) Periconceptional maternal folic acid use of 400 microg per day is related to increased methylation of the IGF2 gene in the very young child. *PLoS ONE* **4,** e7845
11. Hoyo, C., Murtha, A. P., Schildkraut, J. M., Jirtle, R. L., Demark-Wahnefried, W., Forman, M. R., Iversen, E. S., Kurtzberg, J., Overcash, F., Huang, Z., and Murphy, S. K. (2011) Methylation variation at IGF2 differentially methylated regions and maternal folic acid use before and during pregnancy. *Epigenetics* **6,** 928–936
12. Girardot, M., Feil, R., and Lleres, D. (2013) Epigenetic deregulation of genomic imprinting in humans: causal mechanisms and clinical implications. *Epigenomics* **5,** 715–728
13. Chang, H., Zhang, T., Zhang, Z., Bao, R., Fu, C., Wang, Z., Bao, Y., Li, Y., Wu, L., Zheng, X., and Wu, J. (2011) Tissue-specific distribution of aberrant DNA methylation associated with maternal low-folate status in human neural tube defects. *J. Nutr. Biochem.* **22,** 117–127
14. Fryer, A. A., Emes, R. D., Ismail, K. M., Haworth, K. E., Mein, C., Carroll, W. D., and Farrell, W. E. (2011) Quantitative, high-resolution epigenetic profiling of CpG loci identifies associations with cord blood plasma homocysteine and birth weight in humans. *Epigenetics* **6,** 86–94
15. Binder, A. M., and Michels, K. B. (2013) The causal effect of red blood cell folate on genome-wide methylation in cord blood: a mendelian randomization approach. *BMC Bioinformatics* **14,** 353
16. Barker, D. J. (1998) In utero programming of chronic disease. *Clin. Sci. (Lond.)* **95,** 115–128
17. Zaghouani, H., Hoeman, C. M., and Adkins, B. (2009) Neonatal immunity: faulty T-helpers and the shortcomings of dendritic cells. *Trends Immunol.* **30,** 585–591
18. Reinius, L. E., Acevedo, N., Joerink, M., Pershagen, G., Dahlen, S. E., Greco, D., Söderhäll, C., Scheynius, A., and Kere, J. (2012) Differential DNA methylation in purified human blood cells: implications for cell lineage and studies on disease susceptibility. *PLoS ONE* **7,** e41361
19. Martino, D. J., Tulic, M. K., Gordon, L., Hodder, M., Richman, T., Metcalfe, J., Prescott, S. L., and Saffery, R. (2011) Evidence for age-related and individual-specific changes in DNA methylation profile of mononuclear cells during early immune development in humans. *Epigenetics* **6,** 1085–1094
20. Chen, Y. A., Lemire, M., Choufani, S., Butcher, D. T., Grafodatskaya, D., Zanke, B. W., Gallinger, S., Hudson, T. J., and Weksberg, R. (2013) Discovery of cross-reactive probes and polymorphic CpGs in the Illumina Infinium HumanMethylation450 microarray. *Epigenetics* **8,** 203–209
21. Leek, J. T., and Storey, J. D. (2007) Capturing heterogeneity in gene expression studies by surrogate variable analysis. *PLoS Genet.* **3,** 1724–1735
22. Jaffe, A. E., Murakami, P., Lee, H., Leek, J. T., Fallin, M. D., Feinberg, A. P., and Irizarry, R. A. (2012) Bump hunting to identify differentially methylated regions in epigenetic epidemiology studies. *Int. J. Epidemiol.* **41,** 200–209
23. Gueant, J. L., Namour, F., Gueant-Rodriguez, R. M., and Daval, J. L. (2013) Folate and fetal programming: a play in epigenomics? *Trends Endocrinol. Metab.* **24,** 279–289
24. Sie, K. K., Li, J., Ly, A., Sohn, K. J., Croxford, R., and Kim, Y. I. (2013) Effect of maternal and postweaning folic acid supplementation on global and gene-specific DNA methylation in the liver of the rat offspring. *Mol. Nutr. Food Res.* **57,** 677–685
25. Zuo, X., Sheng, J., Lau, H. T., McDonald, C. M., Andrade, M., Cullen, D. E., Bell, F. T., Iacovino, M., Kyba, M., Xu, G., and Li, X. (2012) Zinc finger protein ZFP57 requires its co-factor to recruit DNA methyltransferases and maintains DNA methylation imprint in embryonic stem cells via its transcriptional repression domain. *J. Biol. Chem.* **287,** 2107–2118
26. Quenneville, S., Verde, G., Corsinotti, A., Kapopoulou, A., Jakobsson, J., Offner, S., Baglivo, I., Pedone, P. V., Grimaldi, G., Riccio, A., and Trono, D. (2011) In embryonic stem cells, ZFP57/KAP1 recognize a methylated hexanucleotide to affect chromatin and DNA methylation of imprinting control regions. *Mol. Cell.* **44,** 361–372
27. Plant, K., Fairfax, B. P., Makino, S., Vandiedonck, C., Radhakrishnan, J., and Knight, J. C. (2013) Fine mapping genetic determinants of the highly variably expressed MHC gene ZFP57. *Eur. J. Hum. Genet.* **22,** 568–571
28. Tada, Y., Yamaguchi, Y., Kinjo, T., Song, X., Akagi, T., Takamura, H., Ohta, T., Yokota, T., and Koide, H. (2014) The stem cell transcription factor ZFP57 induces IGF2 expression to promote anchorage-independent growth in cancer cells. [E-pub ahead of print] *Oncogene* doi: 10.1038/onc.2013.599

Received for publication February 13, 2014.
Accepted for publication May 27, 2014.

Genome-wide DNA methylation profiling identifies a folate-sensitive region of differential methylation upstream of *ZFP57*-imprinting regulator in humans

Manori Amarasekera, David Martino, Sarah Ashley, et al.

FASEB J 2014 28: 4068-4076 originally published online June 2, 2014
Access the most recent version at doi:10.1096/fj.13-249029